Real-time RT-PCR analysis

Total cellular RNA was extracted from cultured cells or liver tissue using ISOGEN (Nippon Gene, Tokyo, Japan). Total cellular RNA (2 μg) was used to generate cDNA from each sample using the SuperScript II reverse-transcriptase (Invitrogen). The mRNA expression levels were measured using the Light Cycler PCR and detection system (Roche, Mannheim, Germany) and Light Cycler Fast Start DNA Master SYBR Green I mix (Roche).

Luciferase assays

Luciferase activity was measured using a luminometer, Lumat LB9501 (Promega) and the Bright-Glo Luciferase Assay System (Promega) or the Dual-Luciferase Reporter Assay System (Promega).

Northern and western hybridization

Total cellular RNA was separated by denaturing agarose-formaldehyde gel electrophoresis, and transferred to a nylon membrane. The membrane was hybridized with a digoxigenin-labeled probe specific for the full-length replicon sequence, and subsequently with a probe specific for beta-actin. The signals were detected by chemiluminescence reaction using a Digoxigenin Luminescent Detection Kit (Roche), and visualized by Fluoro-Imager (Roche). For the western blotting, 10 μg of total cell lysate was separated on NuPAGE 4.12% Bis-TrisGel (Invitrogen), and blotted onto an Immobilon PVDF Membrane (Roche). The membrane was incubated with monoclonal antibodies specific for HCV-NS5A (BioDesign, Saco, ME, USA), NS4A (Virogen, Watertown, MA, USA), or beta-actin (Sigma), and detected by a chemiluminescence reaction (BM Chemiluminescence Blotting Substrate; POD, Roche).

Transient-replication assays

A replicon, pRep-Fluc, was transfected into cells and the luciferase activities of the cell lysates were measured serially. To correct the transfection efficiency, each value was divided by the luciferase activity at 4 h after the transfection.

Stable colony formation assays

Cells were transfected with a replicon, pRep-BSD, and were cultured in the presence of 150 μg/mL of BSD (Invitrogen). BSD-resistant cell colonies appeared after ~3 weeks of culture, and were counted.

HCV-JFH1 virus cell culture

An *in-vitro* transcribed HCV-JFH1 RNA[26] was transfected into Huh7.5.1 cells.[27] Naive Huh7.5.1 cells were subsequently infected by the culture supernatant of the JFH1-RNA transfected Huh-7.5.1 cells, and subjected to siRNA or drug treatments. Replication levels of HCV-RNA were quantified by the realtime RT-PCR by using primers that targeted HCV-NS5B region, HCV-JFH1 sense: 5′-TCA GAC AGA GCC TGA GTC CA-3′, and HCV-JFH1 antisense: 5′-AGT TGC TGG AGG GCT TCT GA-3′.

Mice and adenovirus infection

Transgenic mice, CN2-29, inducibly express mRNA for the HCV structural proteins (genotype1b, nucleotides 294–3435) by the Cre/*lox*P switching system.[28] The transgene does not contain full-length HCV 5′-UTR, but shares the target sequence of the shRNA-HCV. Although the transgenic mouse CN2 has been previously reported as expressing higher levels of the viral proteins, the expression levels of the viral core protein in the CN2-29 mice are modest and similar to that in the liver of HCV patients. Thus, we chose CN2-29 mice in the present study.

The mice were infected with AxshRNA-HCV or controls (AxshRNA-Control or AxCAw1) in combination with AxCAN-Cre, which expressed Cre recombinase. Three days after the infection, the mice were killed and HCV core protein in the liver was measured as described below. The BALB/c mice were maintained in the Animal Care Facility of Tokyo Medial and Dental University, and transgenic mice were in the Tokyo Metropolitan Institute of Medical Science. Animal care was in accordance with institutional guidelines. The review board of the university approved our experimental animal studies and all experiments were approved by the institutional animal study committees.

Measurement of HCV core protein in mouse liver

The amounts of HCV core protein in the liver tissue from the mice was measured by a fluorescence enzyme immunoassay (FEIA)[29] with a slight modification. Briefly, the 5F11 monoclonal anti-HCV-core antibody was used as the first antibody on the solid phase, and the 5E3 antibody conjugated with horseradish peroxidase was the second antibody. This FEIA can detect as little as 4 pg/mL of recombinant HCV-core protein. Contents of the HCV core protein in the liver samples were normalized by the total protein contents and expressed as pg/mg total protein.

Immunohistochemical staining

Liver tissue was frozen with optimal cutting temperature (OTC) compound (Tissue Tek; Sakura Finetechnical, Tokyo, Japan). The sections (8 μm thick) were fixed with a 1:1 solution of acetone : methanol at −20°C for 10 min and then washed with phosphate-buffered saline (PBS). Subsequently, the sections were incubated with the IgG fraction of an anti-HCV core rabbit polyclonal antibody (RR8)[28] in blocking buffer or antialbumin rabbit polyclonal antibody (Dako Cytomation, Glostrup, Denmark) in PBS overnight at 4°C. The sections were incubated with secondary antibody, Alexa-antirabbit IgG (Invitrogen) or TRITIC-antirabbit IgG (Sigma), for 2 h at room temperature. Fluorescence was observed using a fluorescence microscope.

Statistical analyses

Statistical analyses were performed using Student's *t*-test; *P*-values of less than 0.05 were considered to be statistically significant.

Results

Retrovirus transduction of shRNA can protect from HCV replication

Retrovirus vectors propagated from pLNCshRNA-HCV and pLNCshRNA-Control were used to infect Huh7 cells, and cell lines were established that constitutively express shRNA-HCV and shRNA-Control (Huh7/shRNA-HCV and Huh7/shRNA-Control, respectively). There were no differences in the cell morphology or growth rate between shRNA-transduced and non-transduced Huh7 cells (data not shown). The HCV replicon, pRep-Fluc, was transfected into Huh7/shRNA-HCV, Huh7/shRNA-Control and naive Huh7 cells by electroporation. In Huh7/shRNA-Control and naive Huh7 cells, the initial luciferase activity at 4 h decreased temporarily, which represents decay of the transfected replicon RNA, but increased again at 48 h and 72 h, which demonstrate de novo synthesis of the HCV replicon RNA. In contrast, transfection into Huh7/shRNA-HCV cells resulted in a decrease in the initial luciferase activity, reaching background by 72 h (Fig. 3a). Similarly, transfection of the replicon, pRep-BSD, into Huh7 cells and BSD selection yielded numerous BSD-resistant colonies in the naive Huh7 (832 colonies) and Huh7/shRNA-Control cell lines (740 colonies), while transfection of Huh7/shRNA-HCV, which expressed shRNA-HCV, yielded obviously fewer colonies (five colonies), indicating reduction of colony forming units by ~10^2 (Fig. 3b). There was no difference in shape, growth or viability between cells expressing the shRNA or not. These results indicated that cells expressing HCV-directed shRNA following retrovirus transduction acquired resistance to HCV replication.

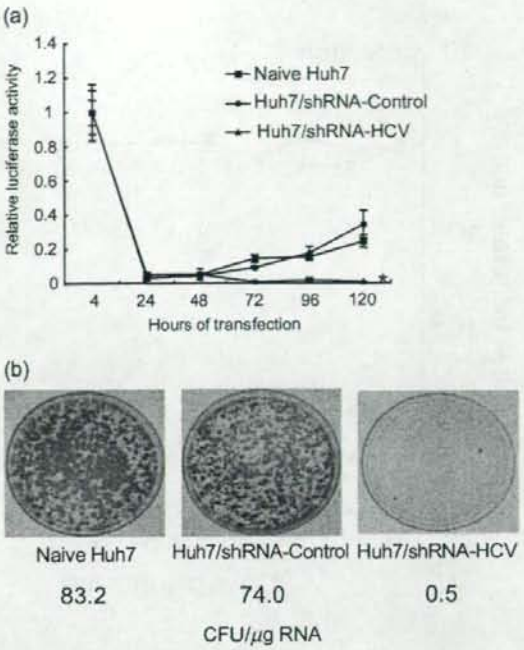

Figure 3 HCV replication can be inhibited by shRNA-HCV which was stably transfected into cells. Huh7/shRNA-HCV and Huh7/shRNA-Control stably express shRNA-HCV or shRNA-Control, respectively, following retroviral transduction. (a) Transient replication assay. An HCV replicon RNA, pRep-Fluc, was transfected into naive Huh7, Huh7/shRNA-HCV and Huh7/shRNA-Control cells. Luciferase activities of the cell lysates were measured serially at the times indicated, and the values were plotted as ratios relative to luciferase activities at 4 h. The luciferase activities at 4 h represent transfected replicon RNA. The data are mean ± SD. An asterisk denotes a *P*-value of less than 0.001 compared with the corresponding value of the naive Huh7 cells. (b) Stable colony formation assay. The HCV replicon, pRep-BSD, was transfected into naive Huh7, Huh7/shRNA-HCV and Huh7/shRNA-Control cells. The cells were cultured in the presence of blasticidin S (BSD) in the medium for ~3 weeks, and the BSD-resistant colonies were counted. These assays were repeated twice. The colony-forming units per microgram RNA (CFU/μg RNA) are shown at the bottom.

Effect of recombinant adenoviruses expressing shRNA on *in vitro* HCV replication

We investigated subsequently the effects of recombinant adenovirus vectors expressing shRNA. AxshRNA-HCV and AxshRNA-Control were used separately to infect Huh7/pRep-Feo cells, and the internal luciferase activities were measured sequentially (Fig. 4a). AxshRNA-HCV caused continuous suppression of HCV RNA replication. Six days postinfection, the luciferase activities fell to background levels. In contrast, the luciferase activities of the Huh7/pRep-Feo cells infected with AxshRNA-Control did not show any significant changes compared with untreated Huh7/pRep-Feo cells (Fig. 4a). The dimethylthiazol carboxymethoxyphenyl sulfophenyl tetrazolium (MTS) assay showed no significant difference between cells that were infected by recombinant adenovirus and uninfected cells (Fig. 4b). In the northern blotting analysis, the cells were harvested 6 days after infection with the adenovirus at an MOI of 1. Feo-replicon RNA of 9.6 kb, which was detectable in the untreated Huh7/pRep-Feo cells and in the cells infected with AxshRNA-Control, diminished substantially following infection with the AxshRNA-HCV (Fig. 4c). Densitometries showed that the intracellular levels of the replicon RNA in the Huh7/pRep-Feo cells correlated well with the internal luciferase activities. Similarly in the western blotting, cells were harvested 6 days after infection with adenovirus. Levels of the HCV NS4A and NS5A proteins that were translated from the HCV replicon decreased following infection with the AxshRNA-HCV (Fig. 4d). These results indicated that the decrease in luciferase activities was due to specific suppressive effects of shRNA on expression of HCV genomic RNA and the viral proteins, and not due to non-specific effects caused by the delivery of shRNA or to toxicity of the adenovirus vectors.

Absence of interferon-stimulated gene responses by siRNA delivery

It has been reported that double-stranded RNA may induce interferon-stimulated gene (ISG) responses which cause instability of mRNA, translational suppression of proteins and apoptotic cell

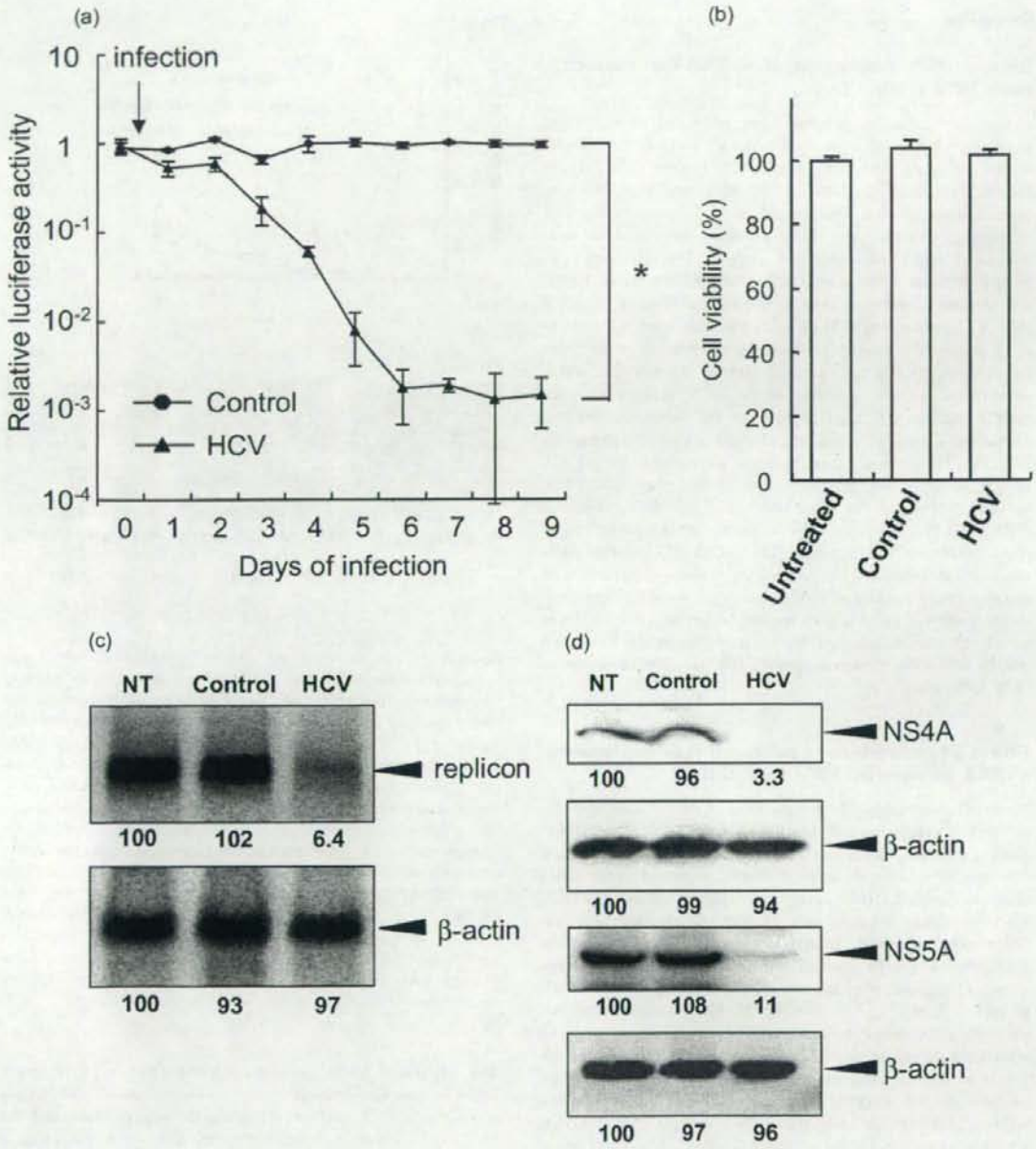

death.[18,30,31] Therefore, we examined the effects of the shRNA-expressing plasmids and adenoviruses on the activation of ISG expression in cells. The ISRE-reporter plasmid, pISRE-TA-Luc, and a control plasmid, peGFPneo, were transfected into Huh7 cells with plasmid pUC19-shRNA-HCV or pUC19-shRNA-Control, or adenovirus, AxshRNA-HCV or AxshRNA-Control, and the ISRE-mediated luciferase activities were measured. On day 2, the ISRE-luciferase activities did not significantly change in cells in which

Journal of Gastroenterology and Hepatology **23** (2008) 1437–1447

Figure 4 Effect of a recombinant adenovirus expressing shRNA on HCV replicon. (a) Huh7/pRep-Feo cells were infected with AxshRNA-HCV or shRNA-Control at a multiplicity of infection (MOI) of 1. The cells were harvested, and internal luciferase activities were measured on day 0 though day 9 after adenovirus infection. Each assay was done in triplicate, and the value is displayed as a percentage of no treatment and as mean ± SD. An asterisk indicates a *P*-value of less than 0.05. (b) Dimethylthiazol carboxymethoxyphenyl sulfophenyl tetrazolium (MTS) assay of Huh7/pRep-Feo cells. Cells were infected with indicated recombinant adenoviruses at an MOI of 1. The assay was done at day 6 of infection. Error bars indicate mean + SD. (c) Northern blotting. The upper panel shows replicon RNA, and the lower panel shows beta-actin mRNA. (d) Western blotting. Total cell lysates were separated on NuPAGE gel, blotted and incubated with monoclonal anti-NS4A or anti-NS5A antibodies. The membrane was re-blotted with antibeta-actin antibodies. NT, untreated Huh7/pRep-Feo cells; Control, cells infected with AxshRNA-Control; HCV, cells treated with AxshRNA-HCV. In panels (b) and (c), cells were harvested on day 6 after adenovirus infection at an MOI of 1.

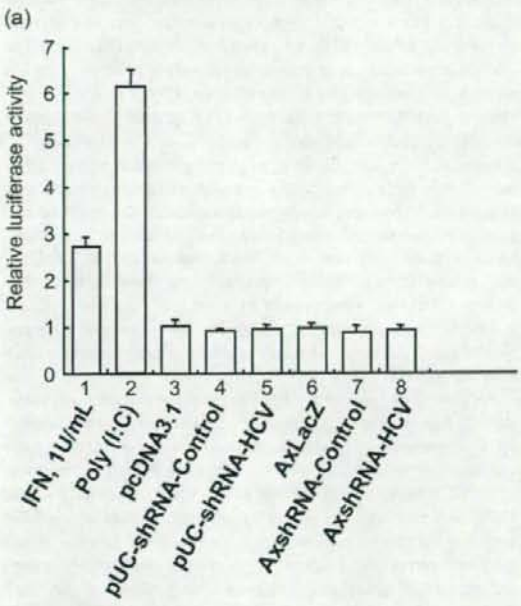

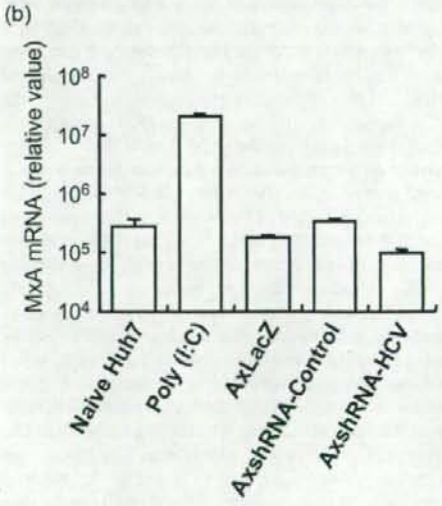

Figure 5 Interferon-stimulated gene responses by transfection of siRNA vectors. (a) Huh7 cells were seeded at 5×10^4 per well in 24-well plates on the day before transfection. As a positive control, 200 ng of pISRE-TA-Luc, or pTA-Luc, 1 ng of pRL-CMV, were transfected into a well using FuGENE-6 Transfection Reagent (Roche), and the cells were cultured with 1 U/mL of interferon (IFN) in the medium (lane 1). Lanes 3–5: 200 ng of pISRE-TA-Luc or pTA-Luc, and 1 ng of pRL-CMV were cotransfected with (lane2) 300 ng of poly (I : C), or 200 ng of plasmids (lane 3) pcDNA3.1, (lane 4) pUC19-shRNA-Control or (lane 5) pUC19-shRNA-HCV. Lanes 6–8: 200 ng of pISRE-TA-Luc or pTA-Luc, and 1 ng of pRL-CMV were transfected, and MOI = 1 of adenoviruses, (lane 6) AxLacZ, which expressed the beta-galactosidase (LacZ) gene under control of the chicken beta-actin (CAG) promoter as a control, (lane 7) AxshRNA-Control or (lane 8) AxshRNA-HCV were infected. Dual luciferase assays were performed at 48 h after transfection. The Fluc activity of each sample was normalized by the respective Rluc activity, and the respective pTA luciferase activity was subtracted from the pISRE luciferase activity. The experiment was done in triplicate, and the data are displayed as means + SD. (b) Huh7 cells were infected with indicated recombinant adenoviruses, AxLacZ, AxshRNA-Control and AxshRNA-HCV. RNA was extracted from each sample at day 6, and mRNA expression levels of an interferon-inducible MxA protein were quantified by the real-time RT-PCR analysis. Primers used were as follows: human MxA sense, 5′-CGA GGG AGA CAG GAC CAT CG-3′; human MxA antisense, 5′-TCT ATC AGG AAG AAC ATT TT-3′; human beta-actin sense, 5′-ACA ATG AAG ATC AAG ATC ATT GCT CCT CCT-3′; and human beta-actin antisense, 5′-TTT GCG GTG GAC GAT GGA GGG GCC GGA CTC-3′.

negative- or positive-control shRNA plasmids was transfected. (Fig. 5a). Similarly, the expression levels of an interferon-inducible MxA protein did not significantly change by transfection of shRNA-expression vectors (Fig. 5b). These results demonstrate that the shRNA used in the present study lack induction of the ISG responses both in the form of the expression plasmids and the adenovirus vectors.

Effect of siRNA and shRNA adenoviruses on HCV-JFH1 cell culture

The effects of HCV-targeted siRNA- and shRNA-expressing adenoviruses were confirmed by using HCV-JFH1 virus cell culture system. Transfection of the siRNA #331[14] into HCV-infected Huh7.5.1 cells resulted in substantial decrease of intracellular HCV RNA, while a control siRNA showed no effect (Fig. 6a). Similarly, infection of AxshRNA-HCV into Huh7.5.1/HCV-JFH1 cells specifically suppressed expression of HCV RNA (Fig. 6b).

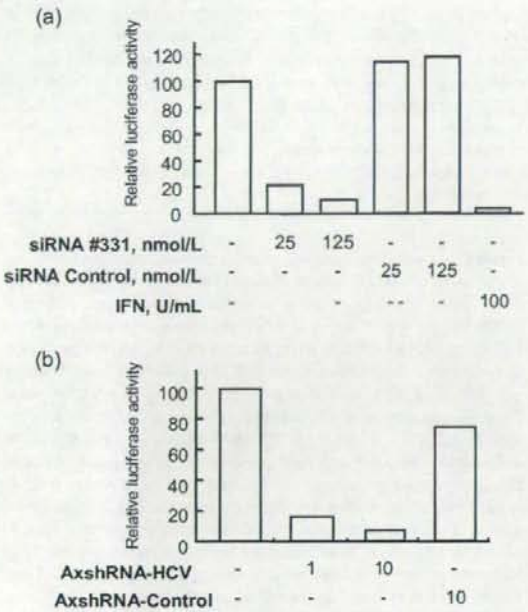

Figure 6 Effects of an siRNA and adenovirus expressing shRNA on HCV-JFH1 cell culture. (a) The siRNA #331, the siRNA-Control[14], (b) AxshRNA-HCV or AxshRNA-Control were, respectively, transfected or infected onto HV-JFH1-infected Huh7.5.1 cells. Seventy-two hours of the transfection or infection, expression level of HCV-RNA was quantified by real-time RT-PCR. The assays were repeated twice, and consistent results were obtained. IFN, recombinant interferon-alpha 2b.

Suppression of HCV-IRES-mediated translation *in vivo* by adenovirus expressing shRNA

The effects of the shRNA expression on the expression of the viral structural proteins *in vivo* were investigated using conditional HCV cDNA-transgenic mice, CN2-29.[28] Adenoviruses, AxshRNA-HCV, AxshRNA-Control or AxCAwI were injected into CN2-29 mice in combination with AxCANCre, an adenovirus expressing *Cre* DNA recombinase. The mice were killed on the fourth day after the injection, and the hepatic expression of the HCV core protein was measured. The expressed amounts of the core protein were 143.0 ± 56.2 pg/mg and 108.5 ± 42.4 pg/mg in AxCAwI and AxshRNA-Control-infected mice, respectively, and the expressed amount was significantly lower in mice injected with AxshRNA-HCV (28.7 ± 7.0 pg/mg, $P < 0.05$, Fig. 7a). Similarly, the induced expression of HCV core protein was not detectable by immunohistochemistry in AxshRNA-HCV infected liver tissue (Fig. 7c). Staining of a host cellular protein, albumin, was not obviously different between the liver infected with AxCAwI, AxshRNA-HCV and AxshRNA-Control (Fig. 7d). The expression levels of two ISG, IFN-beta and Mx1, in the liver tissue were not significantly different between individuals with and without injection of the adenovirus vectors (Fig. 7b). These results indicate specific shRNA silencing of HCV structural protein expression in the liver.

Discussion

The requirements to achieve a high efficiency using RNAi are: (i) selection of target sequences that are the most susceptible to RNAi; (ii) persistence of siRNA activity; and (iii) efficient *in vivo* delivery of siRNA to cells. We have used an shRNA sequence that was derived from a highly efficient siRNA (siRNA331), and constructed a DNA-based shRNA expression cassette that showed competitive effects with the synthetic siRNA (Fig. 2).[14] The shRNA-expression cassette does not only allow extended half-life of the RNAi, but also enables use of gene-delivery vectors, such as virus vectors. As shown in the results, a retrovirus vector expressing shRNA-HCV could stably transduce cells to express HCV-directed shRNA, and the cells acquired protection against HCV subgenomic replication (Fig. 3). An adenovirus vector expressing shRNA-HCV resulted in suppression of HCV subgenomic and protein expression by around three logs to almost background levels (Fig. 4). Consistent results were obtained by using an HCV cell culture (Fig. 6). More importantly, we have demonstrated *in-vivo* effects on viral protein expression in the liver using a conditional transgenic mouse model (Fig. 7). These results suggest that efficient delivery of siRNA could be effective against HCV infection *in vivo*.

An obstacle to applying siRNA technology to treat virus infections is that viruses are prone to mutate during their replication.[32] HCV continuously produces mutated viral strains to escape immune defense mechanisms. Even in a single patient, the circulating HCV population comprises a large number of closely related HCV sequence variants called quasispecies. Therefore, siRNA targeting the protein-coding sequence of the HCV genome, which have been reported by others,[15–19] may vary considerably among different HCV genotypes, and even among strains of the same genotype.[33] Our shRNA sequence targeted the 5′-UTR of HCV RNA, which is the most conserved region among various HCV isolates.[33] In addition, the structural constraints on the 5′-UTR, in terms of its requirement to direct internal ribosome entry and translation of viral proteins, might not permit the evolution of escape mutations. Our preliminary results have shown that the siRNA-HCV suppressed replication of an HCV genotype 2a replicon[34] to the same extent as the HCV 1b replicon.

Although the siRNA techniques rely on a high degree of specificity, several studies report siRNA-induced non-specific effect that may result from induction of ISG responses.[18,31] These effects may be mediated by activation of double-strand RNA-dependent protein kinase, toll-like receptor 3,[35] or possibly by a recently identified RNA helicase, RIG-I.[36] It remains to be determined whether these effects are generally induced by every siRNA construct. Sledz *et al.* have reported that transfection of two siRNA induced cellular interferon responses,[37] while Bridge *et al.* report that shRNA-expressing plasmids induced an interferon response but transfection of synthetic siRNA did not.[31] Speculatively, these effects on the interferon system might be construct dependent. Our shRNA-expression plasmids and adenoviruses did not activate ISG responses *in vitro* (Fig. 5a,b) or *in vivo* (Fig. 7b). We have preliminarily detected phosphorylated PKR (P-PKR) by western

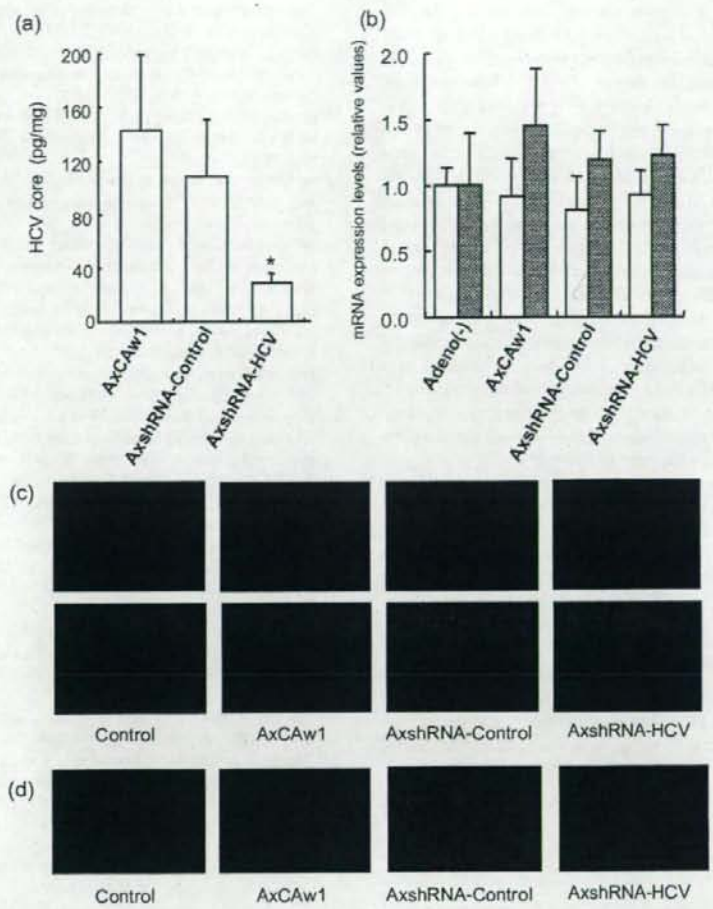

Figure 7 Effects of a recombinant adenovirus expressing shRNA on HCV core protein expression in CN2-29 transgenic mice. CN2-29 transgenic mice were administered with 1×10^9 PFU of AxCANCre combined with 6.7×10^8 PFU of AxshRNA-HCV, AxshRNA or AxCAw1. The mice were killed on day 4 after injection. (a) Quantification of HCV core protein in liver. Liver tissues were homogenized and used to determine the amount of HCV core protein. Each assay was done in triplicate, and the values are displayed as mean ± SD. Asterisk indicates *P*-value of less than 0.05. (b) Expression levels of mouse interferon-beta (white bars) and Mx1 (shaded bars) mRNA in the mouse liver tissue were quantified by the real-time RT-PCR analyses. Primers used were as follows: mouse interferon-beta sense, 5′-ACA GCC CTC TCC ATC AAC TA-3′; mouse interferon-beta antisense, 5′-CCC TCC AGT AAT AGC TCT TC-3′; mouse Mx1 sense, 5′-AGG AGT GGA GAG GCA AAG TC-3′; mouse Mx1 antisense, 5′-CAC ATT GCT GGG GAC TAC CA-3′; mouse beta-actin sense, 5′-ACT CCT ATG TGG GTG ACG AG-3′; mouse beta-actin antisense, 5′-ATA GCC CTC GTA GAT GGG CA-3′. Adeno (-) denotes mice without adenovirus administration. (c) Immunofluorescence microscopy of HCV core protein in the liver tissue. Liver sections of mice were stained using rabbit anticore polyclonal antibody and normal rabbit IgG as a negative control. The upper photographs were obtained at 400× magnification, and the lower photographs were at 1000×. (d) Immunofluorescence microscopy of albumin in liver. Liver sections from the mice were fixed and stained using rabbit antialbumin antibody and normal rabbit IgG as a negative control.

blotting, and found no apparent increase of P-PKR (data not shown). These results indicate that these target sequences and structures are of sufficient specificity to silence the target gene without eliciting non-specific interferon responses.

Beside the canonical action of siRNA, a sequence-specific cleavage of target mRNA, the siRNA could act as a micro-RNA that suppresses translational initiation of mRNA,[38] or it could mediate transcriptional gene silencing.[39] Regarding our *in-vivo* experiments, it was difficult to differentially analyze the effect of siRNA at individual sites of action because post-translational effect of siRNA concomitantly destabilizes target mRNA, which leads to apparent decrease of mRNA transcripts.

Efficiency and safety of gene transfer methods are the key determinants of the clinical success of gene therapy and an unresolved problem. There are several reports of delivery of siRNA or siRNA-expression vectors to cells *in vivo*;[12,40,41] however, gene delivery methods that are safe enough to apply to clinical therapeutics are currently under development. Adenovirus vectors are one of the most commonly used carriers for human gene therapies.[43–44] Our present results demonstrate that the adenoviral delivery of shRNA is effective in blocking HCV replication *in vitro* and virus protein expression *in vivo*. Adenovirus vectors have several advantages of efficient delivery of transgene both *in vitro* and *in vivo* and natural hepatotropism when administered *in vivo*. The AxshRNA-HCV specifically blocked expression of HCV structural proteins in a conditional transgenic mouse expressing those proteins. The current adenovirus vectors may cause inflammatory reactions in the target organ,[45] however, and produce neutralizing antibodies which make repeated administration difficult. These problems may be overcome by the improved constructs of virus vectors with attenuated immunogenicity or by the development of non-viral carriers for gene delivery.[46]

In conclusion, our results demonstrate the effectiveness and feasibility of the siRNA expression system. The efficiency of adenovirus expressing shRNA that target HCV suggests that delivery and expression of siRNA in hepatocytes may eliminate the virus and that this RNA-targeting approach might provide a potentially effective future therapeutic option for HCV infection.

Acknowledgments

This study was supported by grants from Japan Society for the Promotion of Science, 15590629 and 16590580, and partly supported by a grant from the Viral Hepatitis Research Foundation of Japan.

References

1 Alter MJ. Epidemiology of hepatitis C. *Hepatology* 1997; **26**: 62S–65S.
2 Hadziyannis SJ, Sette H Jr, Morgan TR *et al.* Peginterferon-alpha2a and ribavirin combination therapy in chronic hepatitis C: a randomized study of treatment duration and ribavirin dose. *Ann. Intern. Med.* 2004; **140**: 346–55.
3 Fire A, Xu S, Montgomery M, Kostas S, Driver S, Mello C. Potent and specific genetic interference by double-stranded RNA in Caenorhabditis elegans. *Nature* 1998; **19**: 806–11.
4 Elbashir SM, Harborth J, Lendeckel W, Yalcin A, Weber K, Tuschl T. Duplexes of 21-nucleotide RNAs mediate RNA interference in cultured mammalian cells. *Nature* 2001; **411**: 494–8.
5 Coburn GA, Cullen BR. Potent and specific inhibition of human immunodeficiency virus type 1 replication by RNA interference. *J. Virol.* 2002; **76**: 9225–31.
6 Jacque JM, Triques K, Stevenson M. Modulation of HIV-1 replication by RNA interference. *Nature* 2002; **418**: 435–8.
7 Gitlin L, Karelsky S, Andino R. Short interfering RNA confers intracellular antiviral immunity in human cells. *Nature* 2002; **418**: 430–4.
8 Ge Q, Filip L, Bai A, Nguyen T, Eisen HN, Chen J. Inhibition of influenza virus production in virus-infected mice by RNA interference. *Proc. Natl. Acad. Sci. USA* 2004; **101**: 8676–81.
9 Wang C, Pflugheber J, Sumpter R Jr *et al.* Alpha interferon induces distinct translational control programs to suppress hepatitis C virus RNA replication. *J. Virol.* 2003; **77**: 3898–912.
10 Klein C, Bock CT, Wedemeyer H *et al.* Inhibition of hepatitis B virus replication in vivo by nucleoside analogues and siRNA. *Gastroenterology* 2003; **125**: 9–18.
11 Konishi M, Wu CH, Wu GY. Inhibition of HBV replication by siRNA in a stable HBV-producing cell line. *Hepatology* 2003; **38**: 842–50.
12 McCaffrey AP, Meuse L, Pham TT, Conklin DS, Hannon GJ, Kay MA. RNA interference in adult mice. *Nature* 2002; **418**: 38–9.
13 Shlomai A, Shaul Y. Inhibition of hepatitis B virus expression and replication by RNA interference. *Hepatology* 2003; **37**: 764–70.
14 Yokota T, Sakamoto N, Enomoto N *et al.* Inhibition of intracellular hepatitis C virus replication by synthetic and vector-derived small interfering RNAs. *EMBO Rep.* 2003; **4**: 602–8.
15 Kapadia SB, Brideau-Andersen A, Chisari FV. Interference of hepatitis C virus RNA replication by short interfering RNAs. *Proc. Natl. Acad. Sci. USA* 2003; **100**: 2014–18.
16 Kronke J, Kittler R, Buchholz F *et al.* Alternative approaches for efficient inhibition of hepatitis C virus RNA replication by small interfering RNAs. *J. Virol.* 2004; **78**: 3436–46.
17 Randall G, Grakoui A, Rice CM. Clearance of replicating hepatitis C virus replicon RNAs in cell culture by small interfering RNAs. *Proc. Natl. Acad. Sci. USA* 2003; **100**: 235–40.
18 Seo MY, Abrignani S, Houghton M, Han JH. Letter to the editor: small interfering RNA-mediated inhibition of hepatitis C virus replication in the human hepatoma cell line Huh-7. *J. Virol.* 2003; **77**: 810–12.
19 Wilson JA, Jayasena S, Khvorova A *et al.* RNA interference blocks gene expression and RNA synthesis from hepatitis C replicons propagated in human liver cells. *Proc. Natl. Acad. Sci. USA* 2003; **100**: 2783–8.
20 Guo JT, Bichko VV, Seeger C. Effect of alpha interferon on the hepatitis C virus replicon. *J. Virol.* 2001; **75**: 8516–23.
21 Tanabe Y, Sakamoto N, Enomoto N *et al.* Synergistic inhibition of intracellular hepatitis C virus replication by combination of ribavirin and interferon-alpha. *J. Infect. Dis.* 2004; **189**: 1129–39.
22 Maekawa S, Enomoto N, Sakamoto N *et al.* Introduction of NS5A mutations enables subgenomic HCV-replicon derived from chimpanzee-infectious HC-J4 isolate to replicate efficiently in Huh-7 cells. *J. Viral. Hepat.* 2004; **11**: 394–403.
23 Miyagishi M, Sumimoto H, Miyoshi H, Kawakami Y, Taira K. Optimization of an siRNA-expression system with an improved hairpin and its significant suppressive effects in mammalian cells. *J. Gene Med.* 2004; **6**: 715–23.
24 Li Y, Yokota T, Matsumura R, Taira K, Mizusawa H. Sequence-dependent and independent inhibition specific for mutant ataxin-3 by small interfering RNA. *Ann. Neurol.* 2004; **56**: 124–9.
25 Kanazawa N, Kurosaki M, Sakamoto N *et al.* Regulation of hepatitis C virus replication by interferon regulatory factor-1. *J. Virol.* 2004; **78**: 9713–20.
26 Wakita T, Pietschmann T, Kato T *et al.* Production of infectious hepatitis C virus in tissue culture from a cloned viral genome. *Nat. Med.* 2005; **11**: 791–6.
27 Zhong J, Gastaminza P, Cheng G *et al.* Robust hepatitis C virus infection in vitro. *Proc. Natl. Acad. Sci. USA* 2005; **102**: 9294–9.
28 Wakita T, Taya C, Katsume A *et al.* Efficient conditional transgene expression in hepatitis C virus cDNA transgenic mice mediated by the Cre/loxP system. *J. Biol. Chem.* 1998; **273**: 9001–6.
29 Kashiwakuma T, Hasegawa A, Kajita T *et al.* Detection of hepatitis C virus specific core protein in serum of patients by a sensitive fluorescence enzyme immunoassay (FEIA). *J. Immunol. Methods* 1996; **28**: 79–89.

30 Baglioni C, Nilsen TW. Mechanisms of antiviral action of interferon. *Interferon* 1983; **5**: 23–42.
31 Bridge A, Pebernard S, Ducraux A, Nicoulaz A, Iggo R. Induction of an interferon response by RNAi vectors in mammalian cells. *Nat. Genet.* 2003; **34**: 263–4.
32 Carmichael GG. Silencing viruses with RNA. *Nature* 2002; **418**: 379–80.
33 Okamoto H, Okada S, Sugiyama Y *et al.* Nucleotide sequence of the genomic RNA of hepatitis C virus isolated from a human carrier: comparison with reported isolates for conserved and divergent regions. *J. Gen. Virol.* 1991; **72**: 2697–704.
34 Kato T, Date T, Miyamoto M *et al.* Efficient replication of the genotype 2a hepatitis C virus subgenomic replicon. *Gastroenterology* 2003; **125**: 1808–17.
35 Alexopoulou L, Holt AC, Medzhitov R, Flavell RA. Recognition of double-stranded RNA and activation of NF-kB by Toll-like receptor 3. *Nature* 2001; **413**: 732–8.
36 Yoneyama M, Kikuchi M, Natsukawa T *et al.* The RNA helicase RIG-I has an essential function in double-stranded RNA-induced innate antiviral responses. *Nat. Immunol.* 2004; **5**: 730–7.
37 Sledz C, Holko M, de Veer M, Silverman R, Williams, B. Activation of the interferon system by short-interfering RNAs. *Nat. Cell. Biol.* 2003; **5**: 834–9.
38 Doench JG, Petersen CP, Sharp PA. siRNAs can function as miRNAs. *Genes Dev.* 2003; **17**: 438–42.
39 Morris KV. siRNA-mediated transcriptional gene silencing: the potential mechanism and a possible role in the histone code. *Cell. Mol. Life Sci.* 2005; **62**: 3057–66.
40 Xia H, Mao Q, Paulson HL, Davidson BL. siRNA-mediated gene silencing in vitro and in vivo. *Nat. Biotechnol.* 2002; **20**: 1006–10.
41 Zender L, Hutker S, Liedtke C *et al.* Caspase 8 small interfering RNA prevents acute liver failure in mice. *Proc. Natl. Acad. Sci. USA* 2003; **100**: 7797–802.
42 Akli S, Caillaud C, Vigne E *et al.* Transfer of a foreign gene into the brain using adenovirus vectors. *Nat. Genet.* 1993; **3**: 224–8.
43 Bajocchi G, Feldman SH, Crystal RG, Mastrangeli A. Direct in vivo gene transfer to ependymal cells in the central nervous system using recombinant adenovirus vectors. *Nat. Genet.* 1993; **3**: 229–34.
44 Davidson BL, Allen ED, Kozarsky KF, Wilson JM, Roessler BJ. A model system for in vivo gene transfer into the central nervous system using an adenoviral vector. *Nat. Genet.* 1993; **3**: 219–23.
45 Yang Y, Wilson JM. Clearance of adenovirus-infected hepatocytes by MHC class I-restricted CD4+ CTLs in vivo. *J. Immunol.* 1995; **155**: 2564–70.
46 Fleury S, Driscoll R, Simeoni E *et al.* Helper-dependent adenovirus vectors devoid of all viral genes cause less myocardial inflammation compared with first-generation adenovirus vectors. *Basic Res. Cardiol.* 2004; **99**: 247–56.

Available online at www.sciencedirect.com
ScienceDirect
VIROLOGY
Virology 371 (2008) 71–85
www.elsevier.com/locate/yviro

Development of plaque assays for hepatitis C virus-JFH1 strain and isolation of mutants with enhanced cytopathogenicity and replication capacity

Yuko Sekine-Osajima [a,1], Naoya Sakamoto [a,b,*,1], Kako Mishima [a], Mina Nakagawa [a,b], Yasuhiro Itsui [a], Megumi Tasaka [a], Yuki Nishimura-Sakurai [a], Cheng-Hsin Chen [a], Takanori Kanai [a], Kiichiro Tsuchiya [a], Takaji Wakita [c], Nobuyuki Enomoto [d], Mamoru Watanabe [a]

[a] *Department of Gastroenterology and Hepatology, Tokyo Medical and Dental University, Tokyo, Japan*
[b] *Department for Hepatitis Control, Tokyo Medical and Dental University, Tokyo, Japan*
[c] *Department of Virology II, National Institute of Infectious Diseases, Tokyo, Japan*
[d] *First Department of Internal Medicine, University of Yamanashi, Yamanashi, Japan*

Received 15 June 2007; returned to author for revision 10 July 2007; accepted 9 September 2007
Available online 22 October 2007

Abstract

HCV culture *in vitro* results in massive cell death, which suggests the presence of HCV-induced cytopathic effects. Therefore, we investigated its mechanisms and viral nucleotide sequences involved in this effect using HCV-JFH1 cell culture and a newly developed HCV plaque assay technique. The plaque assay developed cytopathic plaques, depending on the titer of the inoculum. In the virus-infected cells, the ER stress markers, GRP78 and phosphorylated eIF2-alpha, were overexpressed. Cells in the plaques were strongly positive for an apoptosis marker, annexin V. Isolated virus subclones from individual plaque showed greater replication efficiency and cytopathogenicity than the parental virus. The plaque-purified virus had 9 amino acid substitutions, of which 5 were clustered in the C terminal of the NS5B region. Taken together, the cytopathic effect of HCV infection involves ER-stress-induced apoptotic cell death. Certain HCV genomic structures may determine the viral replication capacity and cytopathogenicity.

Keywords: HCV-JFH1; HCV cell culture; Plaque assay; ER stress; Unfolded protein responses; Apoptosis; NS5B RNA-dependent RNA polymerase

Introduction

Molecular analyses of the HCV life cycle, virus–host interactions, and mechanisms of liver cell damage by the virus are not understood completely, mainly because of the lack of cell culture systems. These problems have been partly overcome by the development of the HCV subgenomic replicon (Lohmann et al., 1999) and HCV cell culture systems (Lindenbach et al., 2005; Wakita et al., 2005; Zhong et al., 2005). The HCV-JFH1 strain, which is a genotype 2a clone derived from a Japanese fulminant hepatitis patient that can replicate efficiently in Huh7 cells (Kato et al., 2003; Kato et al., 2001), has contributed to the establishment of the HCV cell culture system. Furthermore, the Huh7-derived cell lines, Huh-7.5 cells, Huh-7.5.1, and Lunet cells allow production of higher viral titers and have a higher permissiveness for HCV (Koutsoudakis et al., 2007; Lindenbach et al., 2005; Zhong et al., 2005). The HCV-JFH1 cell culture system now allows us to study the complete HCV life cycle: virus–cell entry, translation, protein processing, RNA replication, virion assembly, and virus release.

HCV belongs to the family *Flaviviridae*. One of the characteristics of the *Flaviviridae* is that they cause cytopathic effects (CPE). The viruses have positive strand RNA genomes of ~10 kilobases that encode a polyprotein of ~3000 amino acids.

Abbreviations: HCV, hepatitis C virus; IFN, interferon; CPE, cytopathic effect; ER, endoplasmic reticulum; UPR, unfolded protein response; PFU, plaque-forming unit; FFU, focus-forming unit; RdRp, RNA-dependent RNA polymerase.

* Corresponding author. Department of Gastroenterology and Hepatology, Tokyo Medical and Dental University, 1-5-45 Yushima, Bunkyo-ku, Tokyo 113-8519, Japan. Fax: +81 3 5803 0268.
E-mail address: nsakamoto.gast@tmd.ac.jp (N. Sakamoto).
[1] Y.S. and N.S. contributed equally to this work.

0042-6822/$ - see front matter © 2007 Elsevier Inc. All rights reserved.
doi:10.1016/j.virol.2007.09.019

The protein is post-translationally processed by cellular and viral proteases into at least 10 mature proteins. The viral nonstructural proteins accumulate in the ER and direct genomic replication and viral protein synthesis (Bartenschlager and Lohmann, 2000; Jordan et al., 2002; Mottola et al., 2002). It has been reported that Japanese encephalitis virus (JEV), bovine viral diarrhea virus (BVDV), and dengue viruses (DEN) cause apoptotic cell death (Despres et al., 1996; He, 2006; Jordan et al., 2002; Su et al., 2002). In addition, certain amino acid substitutions in the viral structural or nonstructural proteins affect the replication and cytopathogenicity of these viruses substantially (Blight et al., 2000; Maekawa et al., 2004; Mendez et al., 1998). It has been recently reported that HCV-JFH1-transfected Huh-7.5.1 cells died when all of the cells were infected and intracellular HCV-RNA reached maximum levels (Zhong et al., 2006). These findings suggest HCV-induced cytopathogenicity. However, the mechanisms have not been well documented.

In the present study, we investigated the cellular effects of HCV infection and replication using the HCV-JFH1 cell culture system. Here, we report that HCV-JFH1-transfected and infected cells show substantial CPE that are characterized by massive apoptotic cell death with the expression of several ER stress-induced proteins. Taking advantage of the CPE, we developed a plaque assay for HCV in cell culture and isolated subclones of HCV that showed enhanced replication and cytopathogenicity. We have demonstrated that these viral characters were determined by mutations at certain positions in the structural and nonstructural regions of the HCV genome, especially the NS5B region.

Results

Production of infectious HCV-JFH1 by JFH1-RNA transfected cells

After transfection of HCV-JFH1 RNA into Huh-7.5.1 cells, intracellular HCV RNA and HCV antigen were continuously detectable in the cell culture (Fig. 1A). Furthermore, the culture supernatant from the transfected cells was positive for core protein, which reached maximum levels at 14 days post-transfection and was continuously detectable during the cell culture (Fig. 1A, black bar). The culture supernatant was readily infectable to naive Huh-7.5.1 cells (data not shown). Immunofluorescence assay showed that 48% of the JFH1-RNA-transfected cells and 42% of the virus-infected cells were positive for HCV core protein. These results demonstrate that the transcript of HCV-JFH1 clone replicates efficiently and produces infectious virus particles in cells, as reported previously (Wakita et al., 2005; Zhong et al., 2005).

Hepatitis C virus infection induced cytopathic effects in vitro

By the seventh day post-transfection, the production of virus decreased concomitant with massive cell death and then cell growth gradually recovered. At 14–16 days post-transfection, the levels of HCV-RNA and core antigen reached maximum (Fig. 1). In the JFH1 mutants JFH1/GND and JFH1/ΔE1-E2-RNA-transfected Huh-7.5.1 cells, the viral replication and host cell death were not observed. The massive cell death after HCV-

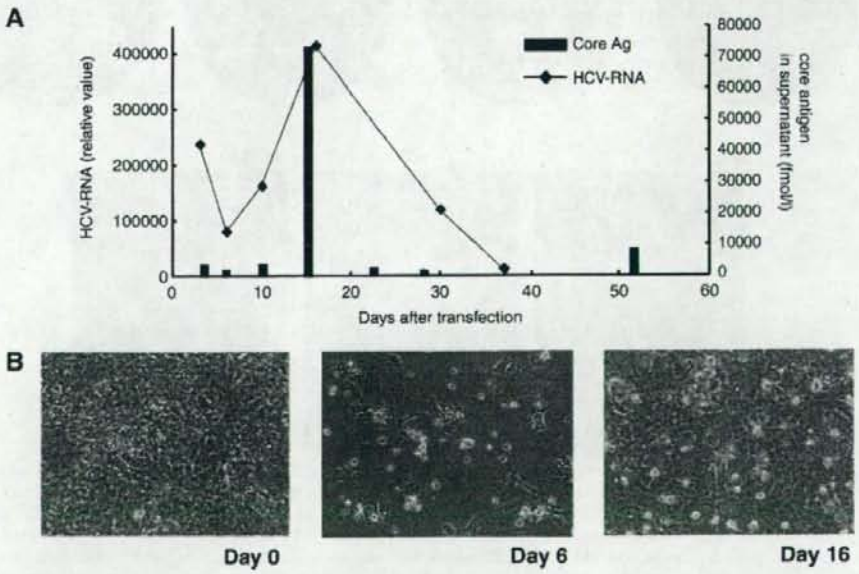

Fig. 1. Replication of HCV-JFH1 RNA in JFH1-transfected and infected Huh-7.5.1 cells. (A) Levels of HCV-RNA in JFH1 RNA-transfected cells. After transfection of the *in vitro* transcribed JFH1-RNA into Huh-7.5.1 cells, total cellular RNA was isolated on indicated days and quantified by real-time RT-PCR. Furthermore, the culture supernatant of JFH1-RNA transfected Huh-7.5.1 cells was collected on the days indicated and the levels of core antigen in the culture supernatant were measured (black bar). (B) HCV-JFH1-transfected Huh-7.5.1 cells (the left panel, day 0; the middle panel, day 6; the right panel, day 16).

JFH1 transfection led us to suspect the occurrence of CPE, produced in host cells by HCV infection and replication. A plaque assay was performed (see Materials and methods) to investigate the morphological CPE following HCV-JFH1 infection. Culture supernatants from JFH1-transfected cells were diluted serially and inoculated onto uninfected Huh-7.5.1

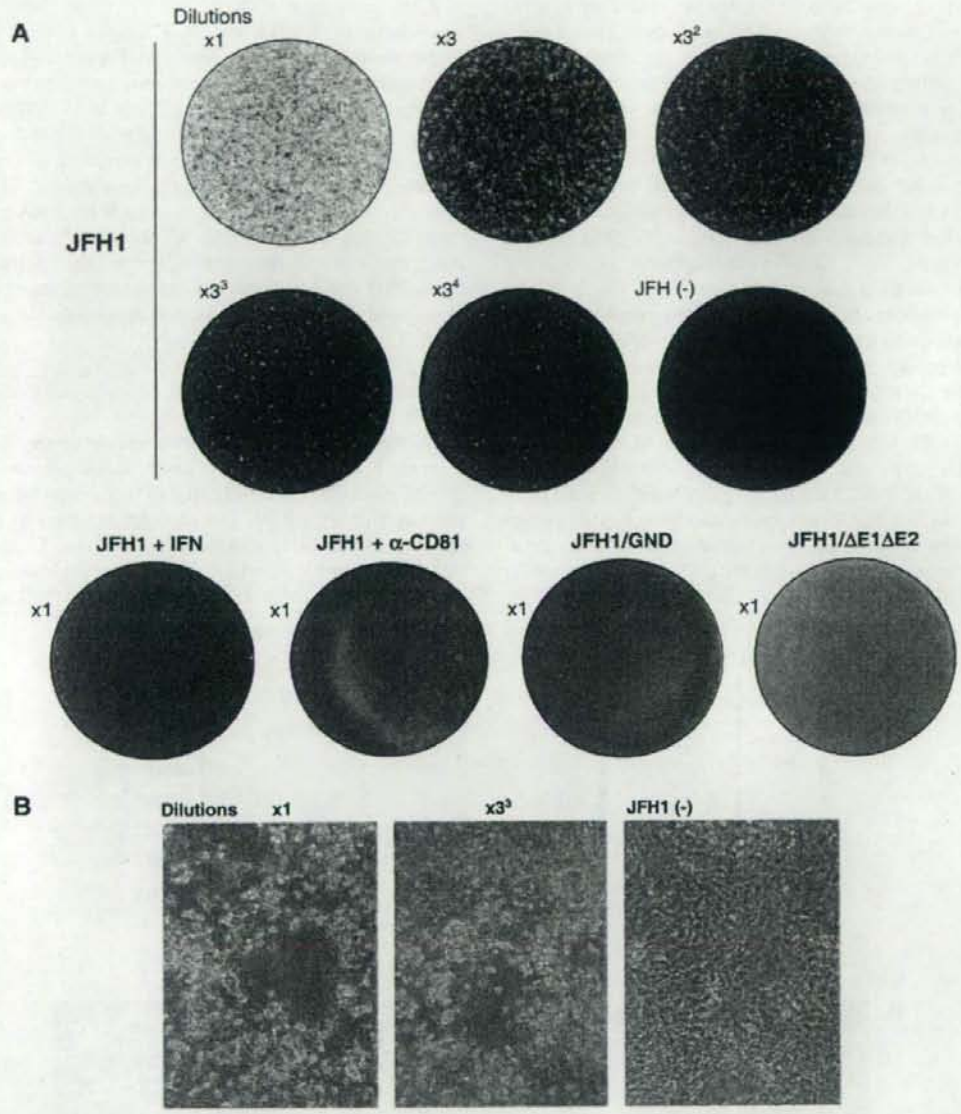

Fig. 2. The cytopathic effects of HCV-JFH1 *in vitro*. (A) Plaque assay. Upper panel, Huh-7.5.1 cells were seeded in collagen-coated 60-mm-diameter plates at density of 4×10^5 cells per plates and were incubated at 37 °C under 5.0% CO_2 (as described above). After overnight incubation, HCV-infected culture supernatants were serially diluted in a final volume of 2 ml per plates and transferred onto the cell monolayers. After ~5 h of incubation, the inocula were removed and the infected cells were overlaid with 8 ml of culture medium containing 0.8% methylcellulose and incubated under normal conditions. After 7 days culture, formation of cytopathic plaque was visualized by staining with 0.08% crystal violet solution. Lower panel, JFH1+IFN; after infection of the virus supernatant, the cells were cultured in the presence of 50 U/ml interferon-alpha. JFH1+a-CD81, Huh-7.5.1 cells were pretreated with 10 μg/plate of anti-CD81 antibody. After incubation at 37 °C for 30 min, anti-CD81 was removed, the cells were washed with PBS, and the HCV-JFH1 culture supernatant was transferred. After ~5 h incubation, the supernatant was removed and the infected cells were overlaid with 8 ml of culture medium containing 0.8% methylcellulose and controls for the plaque assay were also performed with the JFH1/GND or JFH1/ΔE1-E2 culture supernatant. (B) The cytopathic plaques were observed by phase-contrast microscopy at day 7 after HCV-JFH1 infection.

cells. The cells were subsequently cultured in medium containing agarose. Almost 10 days after the inoculation, viable cells were stained and plaques were visualized (Fig. 2A, upper panel). HCV-inoculated cell cultures developed plaques as unstained areas that were accompanied by round cells in the periphery (Fig. 2B). The formation of cytopathic plaques was not observed in a parental Huh7 cell line (data not shown). Immunocytochemistry of the foci revealed the presence of HCV core-positive cells surrounding the cytopathic plaques (Fig. 3A). Culture of the HCV-inoculated cells in the presence of interferon-alpha (50 U/ml) completely abolished the formation of plaques (Fig. 2A, lower panel). Uninfected Huh-7.5.1 cells (Fig. 2A, upper panel), Huh-7.5.1 cells treated with anti-CD81 antibody before HCV-JFH1 infection and JFH1/GND or JFH1/ΔE1-E2-transfected cell cultures did not develop plaques (Fig. 2A, lower panel). These findings suggest that HCV-infected cells develop cytopathic plaques depending on the quantity of the inoculums and that HCV replication, viral protein expression and the propagation of viral particles were the features of these plaques.

HCV-JFH1 infection induced host-cell apoptosis

We next determined whether the cytopathic effects of HCV-JFH1 replication include process of apoptotic cell death. Cells including plaques were double-stained with annexin V-FITC and PI. The ligand of annexin V, phosphatidylserine, is normally confined to the cytoplasmic leaflets of the plasma membrane. In the early phase of apoptosis, phosphatidylserine is exposed on the outer surface of the plasma membrane, which enables detection of FITC-labeled annexin V. As shown in Fig. 4, the fluorescence of annexin V was observed in the cells around the plaques. Foci of apoptotic cells were scattered in the plaques. On the other hand, the expression of annexin V was slightly detectable in the subgenomic replicon-harboring cells, though they were at the same level as the uninfected Huh-7.5.1 cells and the cell death was not observed. Therefore, the cells that express HCV subgenomic replicons did not induce apoptotic cell death. These findings demonstrate that the cytopathic effects of HCV replication and the particle formation induce apoptotic cell death.

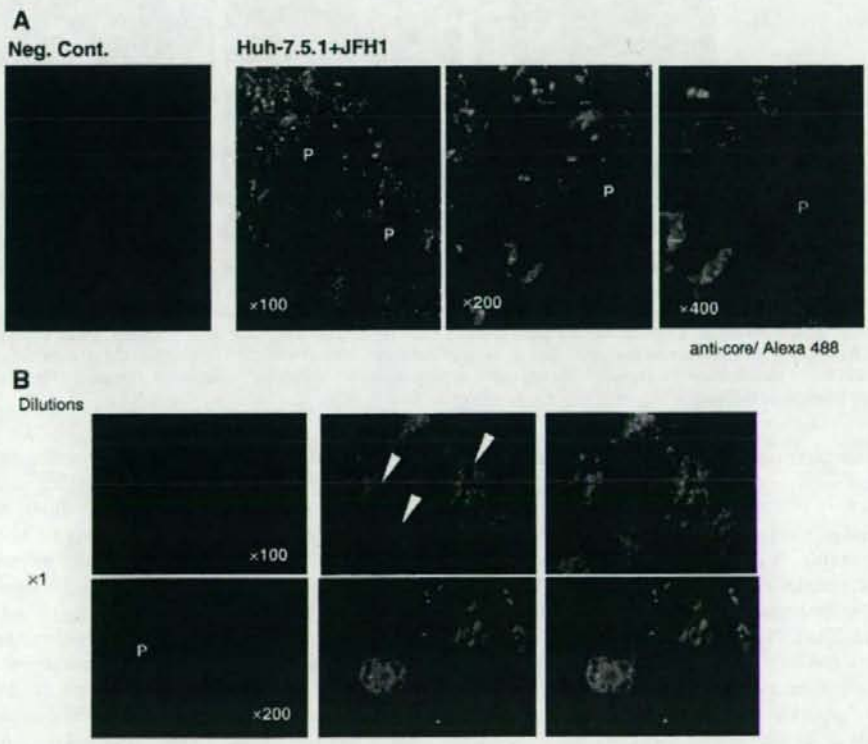

Fig. 3. Immunofluorescence detection of HCV core protein in cytopathic plaques. (A) The HCV-JFH1 culture supernatant was transferred onto uninfected Huh-7.5.1 cells, plated on 22 mm-round micro cover glasses in 60-mm-diameter plates at density of 2×10^5 cells per plate. After ~5 h incubation, the supernatant was replaced with medium containing 0.8% methylcellulose. Immunocytochemistry was performed 12 days after infection. A 'P' indicates a cytopathic plaque. (B) Immunofluorescence detection of HCV-positive foci and cytopathic plaques. The HCV-JFH1 culture supernatant was transferred at various dilutions onto uninfected Huh-7.5.1 cells. After ~5 h incubation, the supernatant was removed and the infected cells were cultured in 60-mm-diameter plate with medium containing 0.8% methylcellulose. Immunocytochemistry was performed 5 days after infection using mouse anti-core antibody. The infectivity and cytotoxicity were quantified by counting HCV-positive foci (FFU/ml) and cytopathic plaque (PFU/ml) respectively. White arrowheads indicate HCV-positive foci.

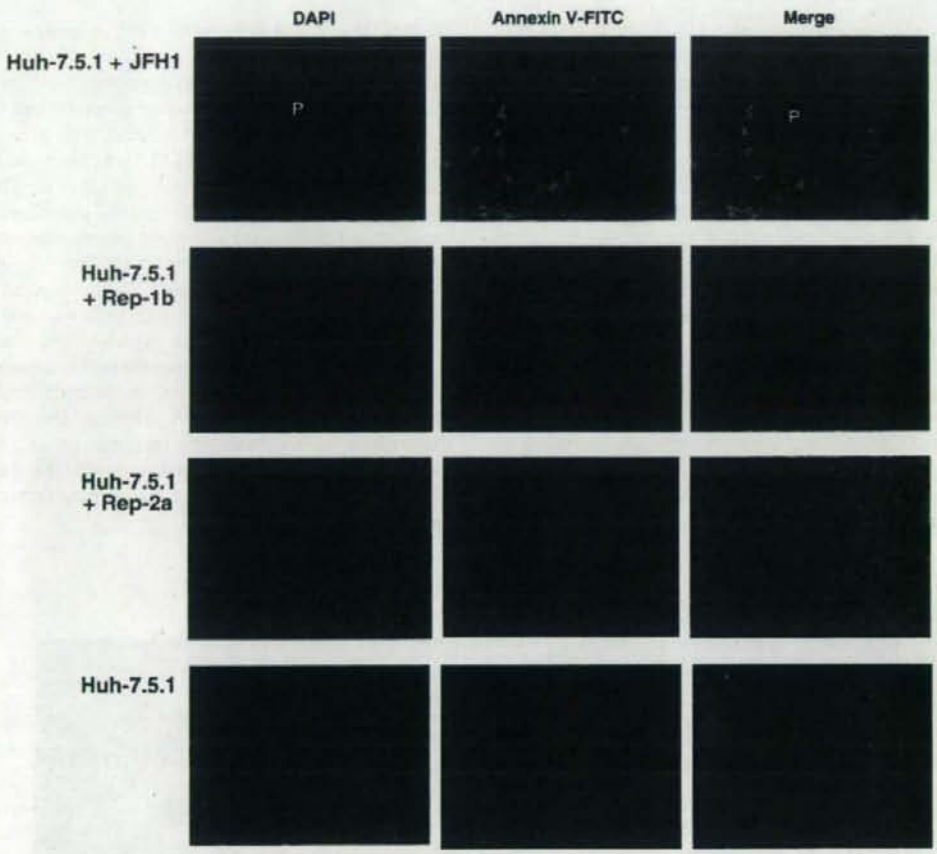

Fig. 4. HCV-JFH1 infection induces apoptosis and leads to plaque formation. The HCV-JFH1 culture supernatant was transferred onto uninfected Huh-7.5.1 cells plated on 22-mm round micro cover glasses in 60-mm-diameter plates at density of 2×10^5 cells per plate. After ~5 h incubation, the supernatant was replaced with medium containing 0.8% methylcellulose. Thirteen days after infection, cover glasses were incubated with 100 μl of staining solution containing Annexin V-FITC at room temperature for 10 to 15 min. The cells that express HCV subgenomic replicons were also incubated and stained with Annexin V-FITC. Rep 1b, Rep-Feo; Rep 2a, SGR-JFH1 (see Materials and methods).

JFH1 replication activates expression of ER stress-related proteins

Cellular stresses such as virus infections prevent protein folding and maturation in the endoplasmic reticulum (ER) and result in the accumulation of misfolded proteins (ER stress) (Kaufman, 1999; Pahl, 1999), triggering the unfolded protein response (UPR). The UPR leads to global shut-off of protein translation and to apoptotic cell death (Ferri and Kroemer, 2001; Mori, 2000; Munro and Pelham, 1986). We and other groups have previously reported that subgenomic or genomic HCV replication induces ER stress and triggers UPR (Nakagawa et al., 2005; Tardif et al., 2002). Therefore, we next studied expression of the ER stress-related proteins, GRP78 and phosphorylated eIF2-alpha, in JFH1-infected cells (Fig. 5). GRP78 is one of the ER chaperones whose expression is induced by ER stress through cleavage and nuclear translocation of ATF6. The eIF2-alpha is phosphorylated by PER-like ER kinase (PERK) on ER stress, causing direct global inhibition of initiation of protein translation (Harding et al., 1999). Huh-7.5.1 cells were infected with HCV-JFH1 supernatant and harvested on the fourth and seventh days post-infection (Fig. 5). As the expression of HCV core protein increased, expression levels of GRP78 and phosphorylated eIF2-alpha also increased substantially. Suppression of virus replication by interferon-alpha treatment led to a decrease of cellular GRP78 and phosphorylated eIF2-alpha. Interferon-alpha treatment did not eliminate the expression of HCV completely, though the levels of core and phosphorylated eIF2-alpha expression apparently decreased compared with the JFH-1 infected Huh-7.5.1 cells at seventh days post-infection. These findings demonstrated that HCV-JFH1 infection induced ER stress.

Persistence of ER stress activates apoptosis signaling pathways, including the induction of C/EBP homologous protein (CHOP) and activation of JNK kinase and caspase12, leading to cell death (Ferri and Kroemer, 2001). As shown in Fig. 5, the

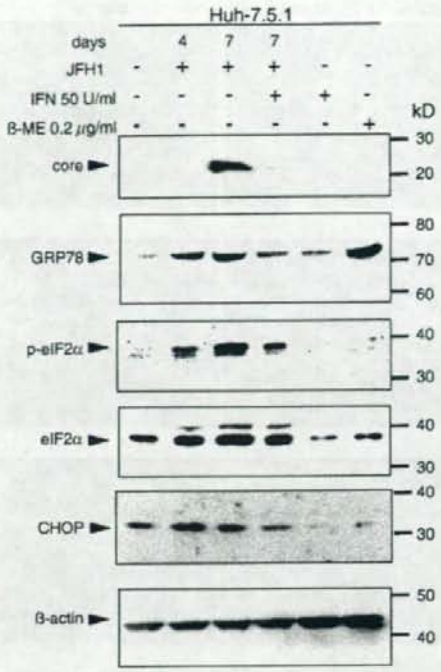

Fig. 5. Expression of ER stress-related proteins in HCV-JFH1 infected cells. The supernatant of JFH1-transfected Huh-7.5.1 cells was transferred onto uninfected Huh-7.5.1 cells. The cells were harvested at 4 and 7 days after infection. The JFH1-infected cells were also cultured with interferon (50 U/ml) or 2-mercaptoethanol (0.2 μg/ml) and harvested after 48 h after treatment. 2-Mercaptoethanol was used as a positive control to induce ER stress (Nakagawa et al., 2005). Western blotting was performed using anti-core, anti-GRP78, anti-phospho-eIF2-alpha (p-eIF2α), anti-eIF2-alpha, anti-GADD153/CHOP, and anti-beta-actin antibodies. β-ME, 2-mercaptoethanol.

level of CHOP expression was apparently increased in JFH1-infected Huh-7.5.1 cells.

To determine whether ER stress contributes to the formation of cytopathic plaques, JFH1-infected cells were incubated in methylcellulose-containing medium and double immunofluorescence staining of the plaques was performed. As shown in Fig. 6, overexpression of GRP78 was colocalized with HCV-core-positive cells with and without CPE. Together with the result shown in Fig. 4, these findings suggest that ER stress is induced in the HCV-JFH1-infected cells and these responses may be involved in development of apoptosis and the formation of cytopathic plaques.

A cytopathic clone could be isolated and this had acquired a high infection efficiency and increased cytopathogenicity

The plaque assay enabled differential quantification of viral infectivity and cytopathogenicity by the immunofluorescence detection of HCV core protein in JFH1-infected, plaque-developed cultures. The number of plaques, as well as infectious foci, was linearly proportional to the dilution of an inoculum (Fig. 7B). It was revealed that only a few populations of HCV-positive foci developed cytopathic plaques (Fig. 3B and Table 1). The infectious focus-forming units and plaque-forming units were 5.6×10^3 FFU/ml and 9.7×10^2 PFU/ml, respectively (Table 1).

To determine whether the difference between the cytopathic and noncytopathic HCV-JFH1 replication might be attributable to viral factors, we isolated clones from each cytopathic plaque. JFH1-infected Huh-7.5.1 cells were incubated in DMEM containing methylcellulose. Cytopathic plaques became visible at ~1 week after inoculation. We isolated cells from each plaque using a cloning cylinder, subcultured, and transferred supernatant onto uninfected Huh-7.5.1 cells. To our surprise, infection of naive cells with plaque-derived supernatants led to massive cell death at 10 days post-infection (Fig. 8A). The supernatant of these cells was transferred again onto uninfected Huh-7.5.1 cells again. Immunofluorescence assay revealed that almost 100% of the cells were positive for HCV core protein (Fig. 8B). The infectivity and cytopathogenicity of this isolated plaque (PI #1) were 4.9×10^3 FFU/ml and 3.0×10^3 PFU/ml respectively (Table 1), much higher than the parental JFH1 clone. Moreover, the ratio of PFU to FFU in a plaque-isolated clone (PI #1) was significantly higher than that of parental JFH1 clone (0.58 and 0.17 respectively) (Table 1 and Figs. 7B and C). We next performed an infection experiment of the parental JFH1 and a plaque-derived clone by adjusting infectious titers of the inocula by HCV core antigen levels. As shown in Fig. 8C, virus from cytopathic plaque (PI #1, #2, #3) showed significantly higher elevation of core antigen levels in supernatants than the parental JFH1 in every time point. The second round isolation of plaques from the PI #1 subclone (PI #1-1, #1-2 and #1-3 in the Table 3) showed consistently higher replication efficiency and cytopathogenicity. These results indicated that JFH1 subclones isolated from cytopathic plaques showed significantly higher infection efficiency and greater cytopathic effects than the original JFH1.

The isolated plaque had amino acid substitutions clustered in the NS5B region

To determine whether there are viral mutations in the cytopathic JFH1 subclone (PI #1), we performed sequence analyses. As shown in Table 2, 11 nucleotide changes were found in the cytopathic plaque, and 9 of these were non-synonymous mutations (81.8%). In particular, 6 of the 11 mutations (9153, 9232, 9293, 9295, 9353, and 9355) were clustered in the C terminal half of the NS5B region. We also performed sequence analyses of the PI #1-isolated subclones, PI #1-1, #1-2, and #1-3, and other clones that had been independently isolated from different plaques, PI #2, #3, and #4 (Table 3). Those subclones showed similar mutations within NS5B region. The C2438S, P2934S, and S3001N substitutions were redundantly appeared in the 4 plaque-isolated clones and in all three PI #1-derived subclones. In contrast, no mutations were found in the virus from infectious foci without plaque formation. These results showed an evidence that certain amino acid mutations were directly associated with the viral replication efficiency and cytopathogenicity.

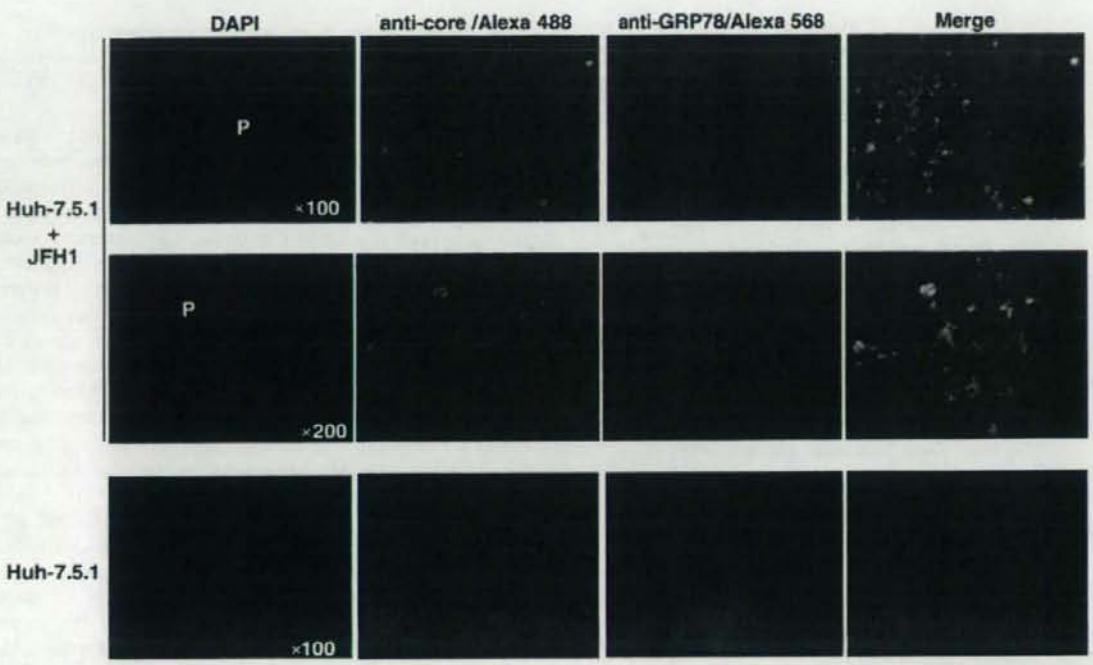

Fig. 6. Co-expression of HCV core and GRP78 in the cytopathic plaque. The HCV-JFH1 culture supernatant was transferred onto uninfected Huh-7.5.1 cells plated on 22-mm round micro cover glasses in 60-mm-diameter plates at density of 4×10^5 cells per plate. After ~5 h incubation, the supernatant was replaced with medium containing 0.8% methylcellulose. Double immunofluorescence was performed 10 days after infection using mouse anti-core antibody and goat-anti-GRP78 antibody.

Introduction of NS5B mutations in JFH1 clone showed higher replication efficiency and cytopathogenicity

We finally investigated on phenotypes of the amino acid mutations identified in the isolated cytopathic subclones. We constructed mutant clones from the wild type JFH1 plasmid, in which three amino acid mutations in NS5B region were individually introduced; T7662A, C9153T, and G9295C (see Tables 2 and 3). Transfection of the mutant HCV-RNAs showed that all mutants developed massive cell death on 10 days after transfection and that their extents of the CPE were apparently greater than the wild type JFH1 clone (Fig. 9A). The levels of core antigen in the culture medium were significantly higher in the mutant clones than in the wild type (Fig. 9B). Furthermore, the expression levels of cellular HCV core protein were significantly higher in the mutant clones than in the wild type with the order of T7662>C9153≫G9295C>JFH1 (Fig. 9C).

Discussions

Our results show that replication of HCV-JFH1 resulted in morphologic changes to the host cells, which are characterized by massive cell death (Figs. 1–3). These observations suggested that HCV infection and replication could cause CPE on the host cells. The development of the CPE involved virus protein-induced ER stress and subsequent apoptotic cell death (Figs. 4–6). The JFH1/ΔE1-E2 with deletion of the HCV envelope proteins-infected Huh-7.5.1 cells did not induce the CPE (Fig. 2A), which indicates that the key factors of plaque formation are not only viral replication but also the propagation of virus particles and re-infection. We took advantage of the HCV-induced CPE and developed a plaque assay using highly permissive Huh-7.5.1 cells. The assay revealed that the HCV-induced cytopathogenicity varied between infectious foci with cytopathic and noncytopathic infection (Fig. 3B). Interestingly, isolated JFH1 subclones from the plaques showed significantly increased infectivity and cytopathogenicity (Table 1 and Fig. 8). Viral genetic analyses showed nine amino acid substitutions; among them five were clustered in the C terminal half of the NS5B region, which might contribute to virus replication efficiency and cytopathogenicity (Table 2).

Cytopathic effects are key characteristics of the *Flaviviridae* that include Japanese encephalitis virus (JEV) (Vaughn and Hoke, 1992), West Nile Virus (Borisevich et al., 2006), yellow fever virus (Quaresma et al., 2006), dengue virus (DEN) (Despres et al., 1993), and bovine viral diarrhea virus (BVDV) (Mendez et al., 1998) and also of viruses such as adenovirus (Shinoura et al., 1999), Epstein–Barr virus (Sato et al., 1989), poliovirus (Yanagiya et al., 2005), and influenza virus (Hinshaw et al., 1994). The *Flaviviridae* utilizes the ER as the primary site for genomic replication and protein synthesis (Jordan et al., 2002; Su et al., 2002; Tardif et al., 2004). It has been reported that apoptotic cell death mediated by virus-induced ER stress contributes to the cytotoxicity of JEV, BVDV, and DEN-2

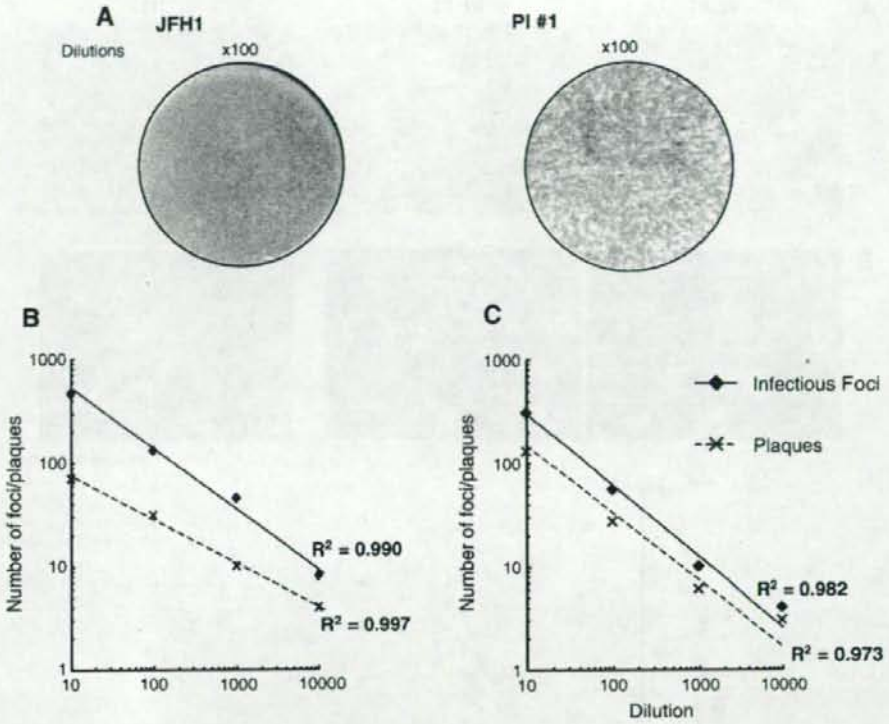

Fig. 7. Correlation of infectious foci or plaques with dilution of an inoculum. (A) Plaque assay. Huh-7.5.1 cells were seeded in collagen-coated 60-mm-diameter plates at density of 4×10^5 cells per plates and were incubated at 37 °C under 5.0% CO_2. After overnight incubation, HCV-JFH1 (left panel) or plaque-purified clone (PI #1) (right panel) infected culture supernatants were serially diluted in a final volume of 2 ml per plates and transferred onto the cell monolayers. After ~5 h of incubation, the inocula were removed, and the cell monolayers were overlaid with 8 ml of culture medium containing 0.8% methylcellulose. After 7 days of culture under normal conditions, formation of cytopathic plaque was visualized by staining with 0.08% crystal violet. (B and C) The PFU-adjusted culture supernatant of parental HCV-JFH1 (B) or plaque-purified clone (PI #1) (C) was transferred at various dilutions onto uninfected Huh-7.5.1 cells, and the plaque assay and immunocytochemistry were performed (described above). The infectivity and cytotoxicity were quantified by counting HCV-positive foci and cytopathic plaque respectively. The horizontal axis showed dilutions of the viral supernatant and the vertical axis showed the number of infectious foci or plaques.

(Jordan et al., 2002; Su et al., 2002; Yu et al., 2006). In DEN-2-infected cells, the NS2B-3 protein causes XBP1 splicing and induces ER stress (Yu et al., 2006). These findings are consistent with our results for HCV in that the JFH1 infection induced ER stress and unfolded protein responses and led to apoptotic cell death and formation of plaques.

The ER is closely associated with viral replication and assembly. Most of the HCV structural and nonstructural proteins accumulate in the ER membrane and form a membranous web that is characterized by a convoluted ER structure (Gosert et al., 2003). Moreover, the folding and assembly of HCV proteins require interaction with ER chaperone proteins such as calreticulin, BiP/GRP78, and heat shock protein-90 (HSP90) (Choukhi et al., 1998; Waxman et al., 2001). The ER stress, which is induced by virus replication, involves three different mechanisms (Tardif et al., 2002): transcriptional induction, translational attenuation, and protein degradation. In our study, both GRP78 and phosphorylated eIF2-alpha proteins were induced as viral proteins increased in concentration in HCV-JFH1 infected cells, and the GRP78 or annexin V and HCV core proteins co-localize in cytopathic plaques, showing that HCV infection and replication induce UPR and that ER stress-mediated apoptosis causes the viral cytopathic effects on host cells.

Table 1
Cytopathogenicity and infectivity of JFH1 clones

	PFU/ml[a]	FFU/ml[b]	PFU/FFU
JFH1	$9.7\pm3.8\times10^2$[c]	$5.6\pm0.9\times10^3$	0.17±0.05
PI #1	$3.0\pm1.9\times10^3$	$4.9\pm1.6\times10^3$	0.58±0.21

[a] PFU, plaque-forming unit.
[b] FFU, focus-forming unit.
[c] Values are displayed as mean±S.D.

Several HCV structural and nonstructural proteins are involved in the ER stress. The structural glycoproteins, E1 and E2, interact with ER chaperones (Choukhi et al., 1998; Liberman et al., 1999), HCV NS4B induces UPR through ATF6 or the IRE1-XBP1 pathway (Zheng et al., 2005), and HCV core triggers apoptosis by inducing ER stress and ER calcium depletion both *in vitro* and *in vivo* (Benali-Furet et al., 2005).

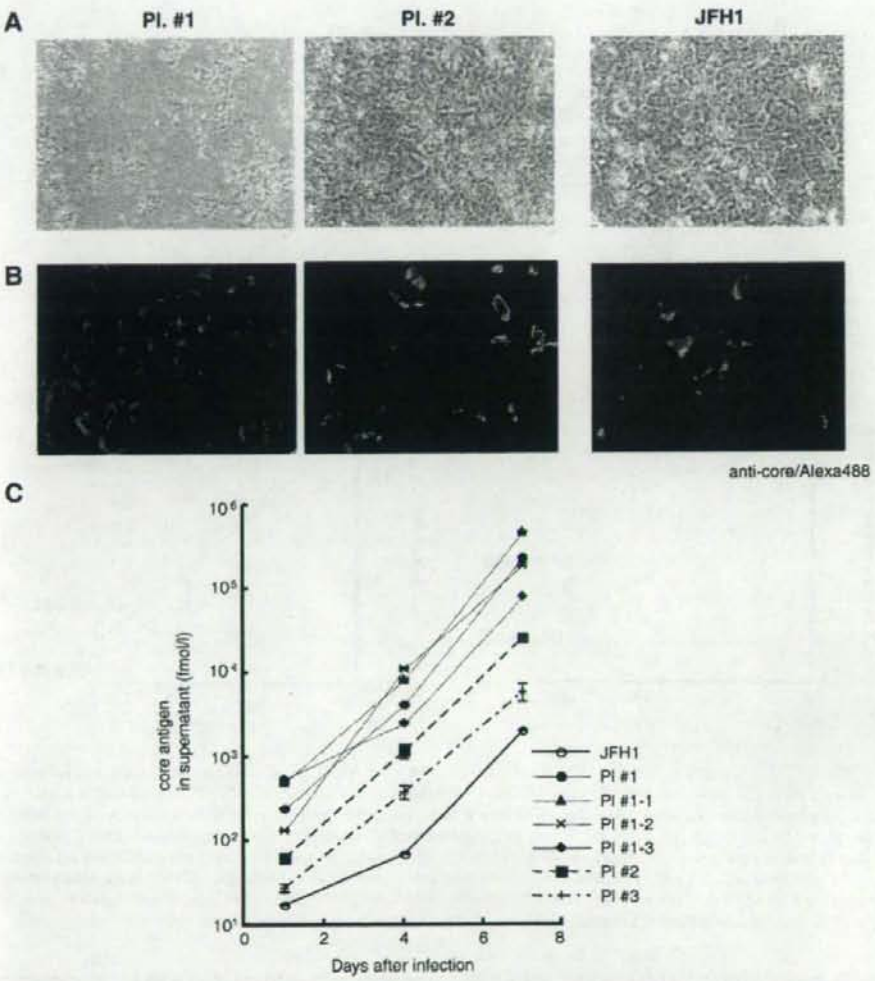

Fig. 8. The isolation of cytopathic plaques. The HCV-JFH1 culture supernatant was transferred at various dilutions onto uninfected Huh-7.5.1 cells. After ~5 h incubation, the supernatant was removed then infected cells were cultured in 0.8% methylcellulose-containing medium in 60-mm-diameter plates. Cytopathic plaques were detectable at 8 days after infection. Cells from each plaque were isolated using a cloning cylinder, subcultured, and transferred onto uninfected Huh-7.5.1 cells. (A) Observation by phase-contrast microscopy at 10 days of culture. (B) After 15 days of culture, the supernatant was transferred onto uninfected Huh-7.5.1 cells and an immunofluorescence assay was performed 5 days after infection using anti-core antibody. (C) Supernatants from parental JFH1, plaque-derived viruses (Pl #1, #2, and #3) and the second round isolation of plaques from the Pl #1 subclones (Pl #1-1, #1-2, and #1-3) were inoculated onto Huh-7.5.1 cells with PFU-adjusted doses, respectively. HCV core antigen levels in culture medium were measured on the days indicated. Inoculation and the assays were done in triplicate. The S.D.s were within 4% in each plot.

HCV E2 induces ER stress at lower levels but binds to PERK and inhibits phosphorylation of eIF2-alpha at high levels of expression (Pavio et al., 2003). These reports have shown that HCV may induce ER stress and regulate subsequent intracellular responses to promote its survival in hepatocytes. Consistently with these reports, our findings that HCV-JFH1 induces the expression of an ER chaperon protein and phosphorylation of eIF2-alpha indicates that robust replication of HCV-JFH1 produces unfolded proteins in the ER, leading to activation of ATF6 and stimulation of the transcription of ER chaperon proteins to promote protein folding. HCV-JFH1-induced unfolded proteins also activate PERK, which phosphorylates eIF2-alpha to inhibit the protein translation. Furthermore, the severe ER stress finally activates apoptosis signaling pathways at the early stage of viral infection. Although which HCV-JFH1 gene product is involved in ER stress-mediated apoptosis is not identified in our study, such proteins may contribute to the regulation of ER stress signaling in the host cell that leads to viral survival or cell death.

The plaque assay is often used to quantify virus infectious titers by visualizing the viral-induced CPE. However, due to the noncytopathic nature of HCV and the lack of highly permissive

Table 2
Nucleotide changes and amino acid substitutions in the cytopathic JFH1 subclone

Nucleotide[a]	Amino acid[a]
A1353G	M334V
C2842A	T843K
G3402A	G1017S
A5819G	Synonymous
T7662A	C2438S
C9153T	P2934S
G9232A	G2960D
G9293C	Synonymous
G9295C	R2985P
C9353A	H3000Q
G9355A	S3001N

[a] Nucleotide and amino acid numbers were derived from pJFH1full (Wakita et al., 2005).

host cell lines, detection of HCV-infected cells commonly relied on visualization of the infected focus by immunostaining HCV proteins (Zhong et al., 2005). Disadvantages include the costs of the antibodies and substrate, additional steps for assay and detection, and microscopic examination to count the foci. By using a highly permissive host cell line and optimizing several conditions, we have developed a plaque assay for HCV. Because the HCV-JFH1 strain is not absolutely cytopathic and does not kill all infected cells, the calculated plaque-forming units do not directly reflect HCV infectious titer but rather reflect cytopathogenicity or the percentage of cytopathic clones in the total infectious foci.

The HCV plaque assay revealed that JFH1 infection and replication developed cytopathic and noncytopathic infectious cell foci (Fig. 3B). One would suspect that the different outcomes of HCV replication might be attributable to the clonal heterogeneity of the host cells. However, there are several pieces of evidence that the Huh-7.5.1 cell line, which we used as host, might be a homogenous cell line. Huh-7.5.1 is derived from parental Huh7 cells through two rounds of clonal selection for neomycin resistance that were dependent on permissiveness for the HCV subgenomic replicon (Blight et al., 2002; Zhong et al., 2005). Sumpter et al. have reported that the HCV-permissive feature is due to mutational inactivation of RIG-I, a cytoplasmic double-stranded RNA sensor that induces type-I IFN production (Sumpter et al., 2005). This evidence suggests that the cytopathic HCV replication is attributable to virus factors, in particular, virus genomic alteration and not by clonal variation or evolution of the host cells.

Indeed, the isolation of the plaque-forming HCV subclones and inoculation onto naive cells showed significantly higher replication yields (Fig. 8) and more frequent development of cytopathic plaques (Table 1). These findings indicate that HCV-JFH1 has evolved into cytopathic and noncytopathic subclones. Our results are similar to BVDV infection. BVDV is divided into two biotypes, cytopathic (*cp*) and noncytopathic (*ncp*) strains. Most *cp* strains, which induce strong apoptotic cell death upon infection, develop from the *ncp* strains by RNA recombination such as insertion of cellular sequences, duplications and rearrangements, and deletions and lead to expression of the NS3 protein (Meyers and Thiel, 1996). Kummerer et al. have reported that other *cp* strain had point mutations in NS2 that enhanced cleavage of NS2/3 junction and NS3 production (Kummerer and Meyers, 2000). As for HCV, considering a rapid HCV replication cycle and the poor fidelity of the viral NS5B RNA-dependent RNA polymerase (RdRp) (Bartenschlager and Lohmann, 2000; Kato et al., 2005), evolution of sequence variants may well develop even after a transfection of cloned HCV-RNA. Very recently, *in vitro* permissive subclones of HCV genotype 1a, H77S stain, have been reported, which have five cell culture-adaptive mutations in the NS3, 4A, and 5A regions (Yi et al., 2007). In these clones, introduction of amino acid substitutions in the p7 and NS2 region enhanced production of the virion particles.

Interestingly, sequence analyses of a cytopathic HCV-JFH1 subclone (Pl #1) identified six amino acid substitutions in the NS5B RdRp (Table 2). Three of the six mutations were redundantly appeared in other clones that were independently isolated from the plaques (Table 3). These findings make us speculate that these amino acid substitutions may affect the enzymatic activity of RdRp by altering tertiary structure of the

Table 3
Nucleotide changes and amino acid substitutions in the NS5B regions of the cytopathic JFH1 subclones

Pl #1	#1-1	#1-2	#1-3	Pl #2	Pl #3	Pl #4
						T7623A (S2428T)
T7662A (C2438S)	T7662A (C2438S)	T7662A (C2438S)	T7662A (C2438S)	T7662A (C2438S)	T7662A (C2438S) A7550C C7551A (N2470T)	
						G8259C C8260G (A2640R)
C9153T (P2934S)	C9153T (P2934S)	C9153T (P2934S)	C9153T (P2934S)		C9153T (P2934S)	
				G9162T (V2941L)		
					A9201T (I2954F)	
G9232A (G2960D)						
				G9235A (R2965Q)		
G9295C (R2985P)	G9295C (R2985P)		G9295C (R2985P)			
C9353A (H3000Q)	C9353A (H3000Q)					
G9355A (S3001N)	G9355A (S3001N)		G9355A (S3001N)			G9355A (S3001N)

Nucleotide and amino acid numbers were derived from pJFH1full (Wakita et al., 2005).

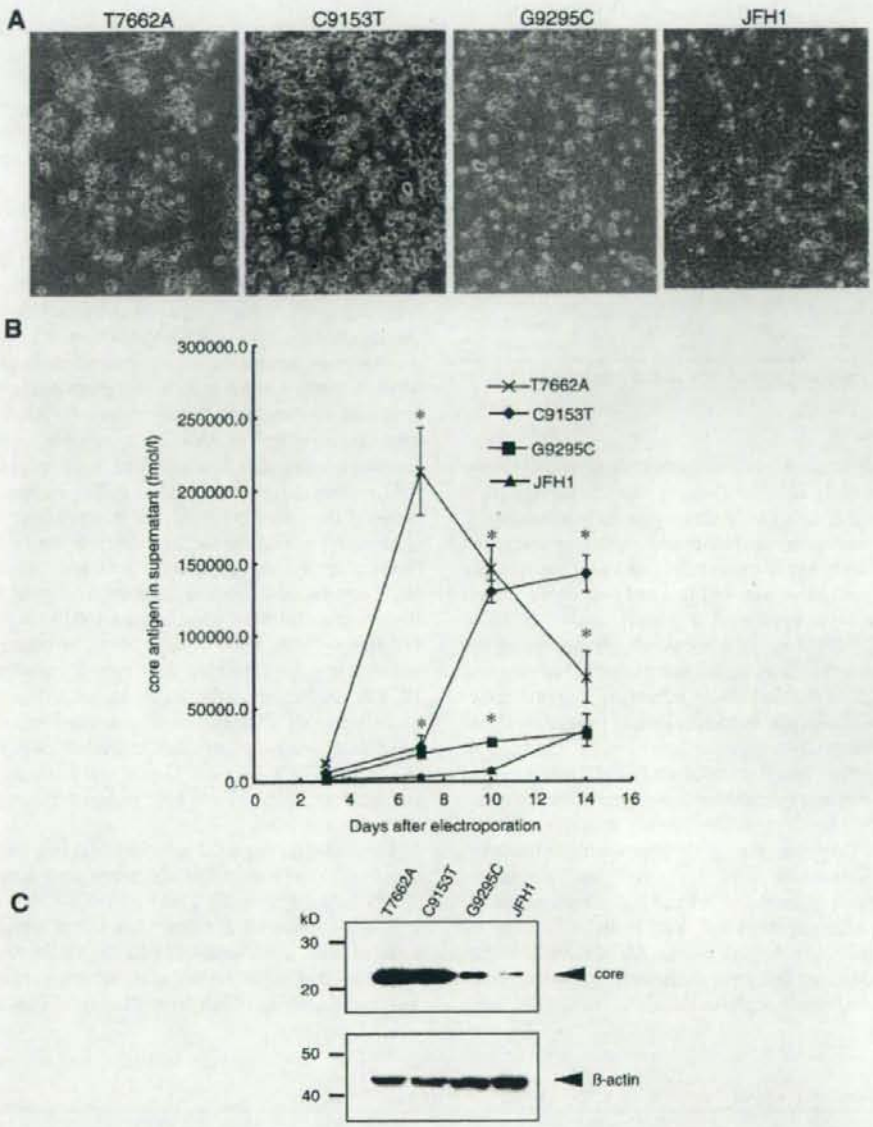

Fig. 9. Introduction of various mutations into the NS5B region of JFH1. The mutations identified in the cytopathic plaque Pl #1; T7662A, C9153T, and G9295C were introduced individually into the parental JFH1. Each JFH1 mutant, T7662A, C9153T, and G9295C, RNA was transfected into Huh-7.5.1 cells by electroporation. The transfected cells were split every 3 to 5 days (see Materials and methods). (A) JFH1 mutants transfected Huh-7.5.1 cells were observed by phase-contrast microscopy at day 7 after transfection. (B) Levels of core antigen in the culture supernatants. The culture supernatants of transfected cells were collected on the days indicated, and the levels of core antigen were measured. Asterisks indicate *p*-values of less than 0.05. (C) The supernatants of JFH1 mutants transfected Huh-7.5.1 cells were transferred onto uninfected Huh-7.5.1 cells. The cells were harvested at 7 days after infection. Western blotting was performed using anti-core and anti-beta-actin.

thumb domain or affect the quaternary structure of the whole HCV replicase complex by altering surface affinity to other nonstructural proteins. Mapping of the amino acid substitutions in the RdRp tertiary structure has shown that the amino acid 2438 was located on the finger domain, and three amino acids, 2934, 2960, and 2985, were located on the outer surface of the thumb domain, which corresponds to the opposite side of the nucleotide tunnel. The other substitutions, 3000 and 3001, were within the domain of the polypeptide linking the polymerase to the membrane anchor (Lesburg et al., 1999). Very

recently, Zhong et al. have reported that long-term culture of HCV-JFH1 of more than 60 days leads to the evolution of certain mutations in the viral genome (Zhong et al., 2006). They identified amino acid changes in Core, E2, NS3, and NS5A regions, and especially E2 mutation increased infectivity and density changes of viruses. In our present study, however, we could not find those mutations in the virus subclones that we have isolated in the plaque assay technique. The discrepancy might be attributable to the presence or absence of HCV-CPE-induced cell clonal alteration of the host Huh-7.5.1 that occurs concomitantly with viral genetic evolution during long-term cell culture. Further analyses may be necessary to determine the most critical regions that regulate the viral replication efficiency and cytopathogenicity.

Interestingly, the mutant virus clones, T7662A (C2438S), C9153T (P2934S), and G9295C (R2985P), showed considerably higher replication efficiency and cytopathogenicity than the wild type JFH1 clone (Fig. 9). These results strongly suggest that certain NS5B mutations in the plaque-purified strains display more replication-efficient and cytopathic phenotypes. The present data are still preliminary. Further studies may be necessary to fully characterize these mutations and their functions, which include introduction of mutations of the HCV region and of the other plaque-purified viruses and combination of the mutations, and to study their effects on virus protein functions. We are at present analyzing derivative JFH1 clones in which other amino acid mutations were introduced.

Several clinical findings have suggested that HCV is not cytopathic and that antiviral immune responses such as cytotoxic T lymphocytes play important roles in HCV pathogenesis (Cerny and Chisari, 1999). On the other hand, apoptotic cell death is the first cellular response to many hepatotoxic events and has been implicated in the pathogenesis of liver diseases, such as viral hepatitis, autoimmune diseases, alcohol-induced injury, cholestasis, hepatocellular carcinoma, and fulminant hepatic failure (Canbay et al., 2004; Ghavami et al., 2005; Patel and Gores, 1995; Rodrigues et al., 2000; Rust and Gores, 2000; Thompson, 1995). Several clinical studies have shown that fulminant hepatic failure (FHF), from which HCV-JFH1 strain was isolated, showed far more hepatocyte apoptosis, as characterized by caspase activation and Fas-FasL expression, than chronic hepatitis and normal populations (Leifeld et al., 2006; Mita et al., 2005; Ryo et al., 2000). The ER stress markers GRP78 and ATF6 are upregulated in the HCV liver tissue as the histological grade advanced. In addition, GRP78 and ATF6 are upregulated as the histological grade increased in hepatocellular carcinoma (HCC) (Shuda et al., 2003) and proteomic analysis of HCC tissue samples has shown significant upregulation of HSP70 and GRP78 (Chuma et al., 2003; Takashima et al., 2003), indicating that these proteins may play important roles in HCV-induced hepatocarcinogenesis.

In conclusion, the cytopathic mutants of HCV-JFH1 strain were isolated by using plaque assay techniques. A mechanism of the cytopathic effects involved ER stress-mediated apoptosis that was triggered by virus infection. That process of cytopathic effects might explain one aspect of HCV-induced liver injury during acute infection. Further analyses of cellular effects on HCV replication may elucidate the pathogenesis of HCV infection and may define novel host factors as targets of antiviral chemotherapeutics.

Materials and methods

Reagents

Recombinant human interferon alpha-2b was from Schering-Plough (Kenilworth, NJ). Beta-mercaptoethanol was from Wako (Osaka, Japan). Anti-CD81 antibody (JS-81) was from BD Biosciences (Franklin Lakes, NJ) (Morikawa et al., 2007).

Cells and cell culture

Huh-7.5.1 cells (Zhong et al., 2005) (kindly provided by Dr Francis V. Chisari) were maintained in Dulbecco's modified minimal essential medium (DMEM, Sigma) supplemented with 2 mmol/l L-glutamine and 10% fetal bovine serum at 37 °C under 5.0% CO_2.

In vitro RNA synthesis and transfection

A plasmid, pJFH1-full (Wakita et al., 2005), which encodes the full-length HCV-JFH1 sequence, and two control plasmids for pJFH1-full were used; pJFH1/GND that is a replication incompetent mutant with a mutation in the NS5B GDD motif and pJFH1/ΔE1-E2 in which a coding region of the HCV envelope proteins was deleted. The HCV RNA was synthesized using the RiboMax Large Scale RNA Production System (Promega, Madison, WI), with the linearized pJFH1 plasmid as template. After DNaseI (RQ-1 RNase-free DNase, Promega) treatment, the transcribed HCV-RNA was purified using ISOGEN (Nippon Gene, Tokyo, Japan). For the RNA transfection, Huh-7.5.1 cells were washed twice, and 5×10^6 cells were resuspended in Opti-MEM I (Invitrogen, Carlsbad, CA) containing 10 μg of HCV RNA, transferred into a 4-mm electroporation cuvette, and subjected to an electric pulse (1050 μF and 270 V) using the Easy Ject system (EquiBio, Mieddlesex, UK). After electroporation, the cell suspension was left for 5 min at room temperature and then incubated under normal culture conditions in a 10-cm diameter cell culture dish. The transfected cells were split every 3 to 5 days. The culture supernatants were subsequently transferred onto uninfected Huh-7.5.1 cells. The levels of HCV replication and viral protein expression were detected by real-time PCR, western blotting, and immunocytochemistry.

HCV subgenomic replicon constructs

HCV subgenomic replicon plasmid pRep-Feo was derived from the HCV-N strain pHCV1bneo-delS (Tanabe et al., 2004) and pSGR-JFH1 was from the HCV-JFH1 strain (Kato et al., 2003). The replicon RNA was synthesized from pRep-Feo or pSGR-JFH1 and transfected into Huh-7.5.1 cells. After culture in the presence of G418 (Wako), cell lines stably expressing the replicon were established.